Materials Research, Vol. 4, No. 3, 149-156, 2001.

Plastic Behavior of Medium Carbon Vanadium Microalloyed Steel at Temperatures Near $\gamma \leftrightarrow \alpha$ Transformation

N.J. Lourenço[a], *A.M. Jorge Jr.*[a], *J.M.A. Rollo*[b], *O. Balancin*[a]*

[a]*Departamento de Engenharia de Materiais, Universidade Federal de São Carlos, São Carlos - SP, Brazil*
[b]*Escola de Engenharia de São Carlos, Universidade de São Paulo, São Carlos - SP, Brazil*

Received: July 7, 2000; Revised: June 28, 2001

Dilatometric techniques were used to build the continuous cooling transformation (CCT) diagram for a medium carbon microalloyed steel; the microstructure and hardness were determined at different cooling rates. The mechanical behavior of the steel in the austenite field and at temperatures approaching austenite to ferrite transformation was measured by means of hot torsion tests under isothermal and continuous cooling conditions. The no recrystallization temperatures, Tnr, and start of phase transformation, Ar_3, were determined under continuous cooling condition using mean flow stress *vs.* inverse of absolute temperature diagrams. Interruption of static recrystallization within the interpass time in the austenite field indicated that the start of vanadium carbonitride precipitation occurred under 860 °C. Austenite transformation was found to start at around 710 °C, a temperature similar to that measured by dilatometry, suggesting that interphase precipitation delays the transformation of deformed austenite. Pearlite was observed at temperatures ranging from 650 °C to 600 °C, with the flow curves taking on a particular shape, *i.e.*, stress rose sharply as strain was increased, reaching peak stress at low deformation, around 0.2, followed by an extensive softening region after peak stress.

Keywords: *microalloyed steel, gamma alpha transformation, hot working*

1. Introduction

Micro additions of carbonitride formers in steels have been widely used in the production of plates, rolled bars and forged components. In conventional thermomechanical treatments of low carbon microalloyed steels, the main goal is to promote austenite grain refinement in the recrystallization temperature range, combined with straining at temperatures below the startup of deformation-induced precipitation. The latter process is very effective because, during low temperature hot deformation, precipitates such as carbonitride particles stabilize the dislocation substructure and retard recrystallization, thus facilitating ferrite refinement. In addition to producing the grain refinement effect, carbonitrides precipitated at austenite–ferrite/pearlite interfaces in medium carbon vanadium microalloyed steels increase the mechanical strength of forged components, producing a precipitation strengthening effect in the range of 150-250 MPa[1]. In addition to increasing their strength, precipitation also decreases the toughness of materials. The toughness of medium carbon pearlite steels can be improved by increasing the ferrite volume fraction and by refining the constituent phases size. Phases constituent refinement may be attained by thermomechanical treatments under warm conditions, at temperatures approaching austenite decomposition[2].

Mechanical tests have been widely used to simulate thermomechanical treatments in the design of conventionally controlled working schedules for medium carbon microalloyed steels[3-5]. To improve the control of austenite grain refinement, double straining tests have been made to investigate the kinetics of static recrystallization[6-8]. The limit between the full static recrystallization region and deformation-induced precipitation has been determined under different deformation conditions by means of multiple pass deformation tests performed under continuous cooling conditions[9,10]. Dilatometric techniques have been employed at austenite decomposition temperatures to determine continuous cooling transformation (CCT) diagrams[11-13]. Although much attention has been focused

* e-mail: balancin@power.ufscar.br

on conventionally controlled work, few systematic studies have been carried out to characterize the plastic behavior of these steels at temperatures close to the gamma alpha transformation.

The purpose of this work was to study the plastic behavior of a medium carbon vanadium microalloyed steel in the austenite field and in the phase transition region. Flow curves were determined under different deformation conditions and the shape and stress levels of these curves were associated with the microstructure present during straining.

2. Material and Experimental Procedures

The material used in this work was a commercial medium carbon vanadium microalloyed forging steel whose chemical composition is given in Table 1. To determine the CCT diagrams, dilatometry tests were carried out using 2 mm diameter, 12 mm long samples. The samples were heated at 2 °C/s up to the soaking temperature of 1150 °C and kept at this temperature for 10 min. Finally, they were cooled down at a rate ranging from 0.2 °C/s to 30 °C/s.

Mechanical tests were carried out on a computerized hot torsion machine[14]. The samples, having a 20 mm length and 6 mm diameter in the reduced central gage section, were heated by means of an infrared furnace mounted directly on the testing machine. Chromel-alumel thermocouples were used to measure and control the temperature. To prevent oxidation, the sample was enclosed in a 2% hydrogen argon atmosphere surrounded by a quartz tube. Data were collected by means of a software program that imposes parameter tests such as strain, strain rate, temperature, and interpass time between straining.

Table 1. Chemical composition of the steel tested (wt%)

C	Si	Mn	V	P	N	Al
0.39	0.62	1.30	0.11	0.016	0.013	0.025

Three kinds of hot torsion tests were performed: isothermal continuous tests, multiple pass tests under continuous cooling conditions, and isothermal double straining tests.

(a) Isothermal continuous tests. These tests were carried out to determine the plastic flow curves at different temperatures. Samples were heated from room temperature to the soaking temperature of 1150 °C, held at this temperature for 10 min, cooled to the test temperature at a rate of 1 °C/s, held for 1 min, and finally strained isothermally until fracture, as illustrated in Figure 1a. These tests were carried out over a temperature range of 600 °C to 1150 °C, and at equivalent strain rates of 0.3, 0.5 and 1.0 s^{-1}.

(b) Multiple pass tests under continuous cooling conditions. The purpose of these tests was to investigate deformation-induced phenomena that may occur upon deformations schedule. Critical temperatures for the hot working process, Tnr and Ar_3, were also determined. For this kind of test, samples were heated from room temperature to a soaking temperature of 1150 °C and kept at this temperature for 10 min, followed by cooling at a rate of 1 °C/s, as indicated in Fig. 1b. The first straining was at 1120 °C and the elapsed time between deformations was 30 s.

(c) Isothermal double straining tests. These experiments were carried out to investigate hardening and softening processes that may occur after hot deformation. The samples were heated from room temperature to a soaking temperature of 1150 °C and maintained at this temperature for 10 min, followed by cooling to test temperature at a rate of 1 °C/s, where they were held for 1 min before the first straining. After this straining followed by an unloading period, a second straining was applied at the same strain rate and temperature, as indicated in Fig. 1c. The interpass time between deformations ranged from 60 to 500 s.

Results

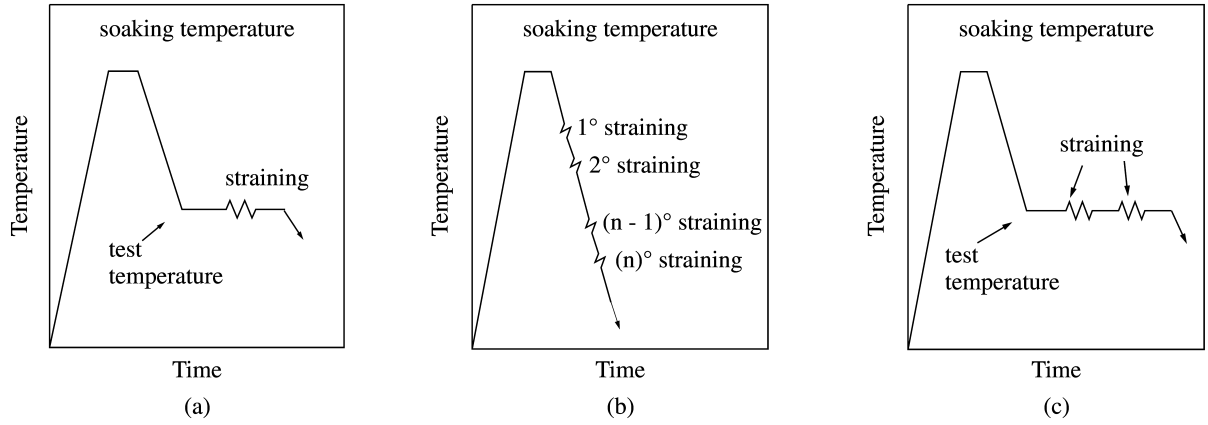

Figure 1. Temperature-time schedules followed in hot torsion tests: isothermal continuous tests (a), multiple pass tests under continuous cooling conditions (b), and isothermal double straining tests (c).

Start and finish transformation temperatures, under the continuous cooling conditions determined by dilatometry tests, are illustrated in the CCT diagram plotted in Fig. 2. The hardness and microstructures observed after cooling to room temperature at each cooling rate applied are also displayed in this figure. These data indicate that, at low cooling rates of less than 2 °C/s, the microstructure is composed of pro-eutectoid ferrite and pearlite. On the other hand, bainite is formed at cooling rates ranging from 5 °C/s to 10 °C/s, while martensite is observed at the highest cooling rates.

The plastic flow curves obtained by isothermal continuous tests with strain rates of 1.0 s^{-1} are displayed in Fig. 3 and indicate that the level of stress depends on deformation temperature. Stress increases as temperature decreases, but this increment is higher at lower temperatures. It is also worth noting that the shape of the flow curves changes as deformation temperature is altered. At high temperatures exceeding 700 °C, the flow curves show the characteristic shape expected for materials that soften by dynamic recrystallization. At lower temperatures, however, the curve has a peculiar shape: rapid work hardening to a hump, followed by an extensive flow-softening region.

In order to emphasize the differences in the shape of the flow curves at high and low temperatures, the dependence of peak stress and peak strain on deformation temperature was determined, as displayed in Figures 4 and 5. In addition, the apparent activation energy was determined using the generalized hot-working relationship between peak stress and strain rate proposed by Sellars and Tegart[15]:

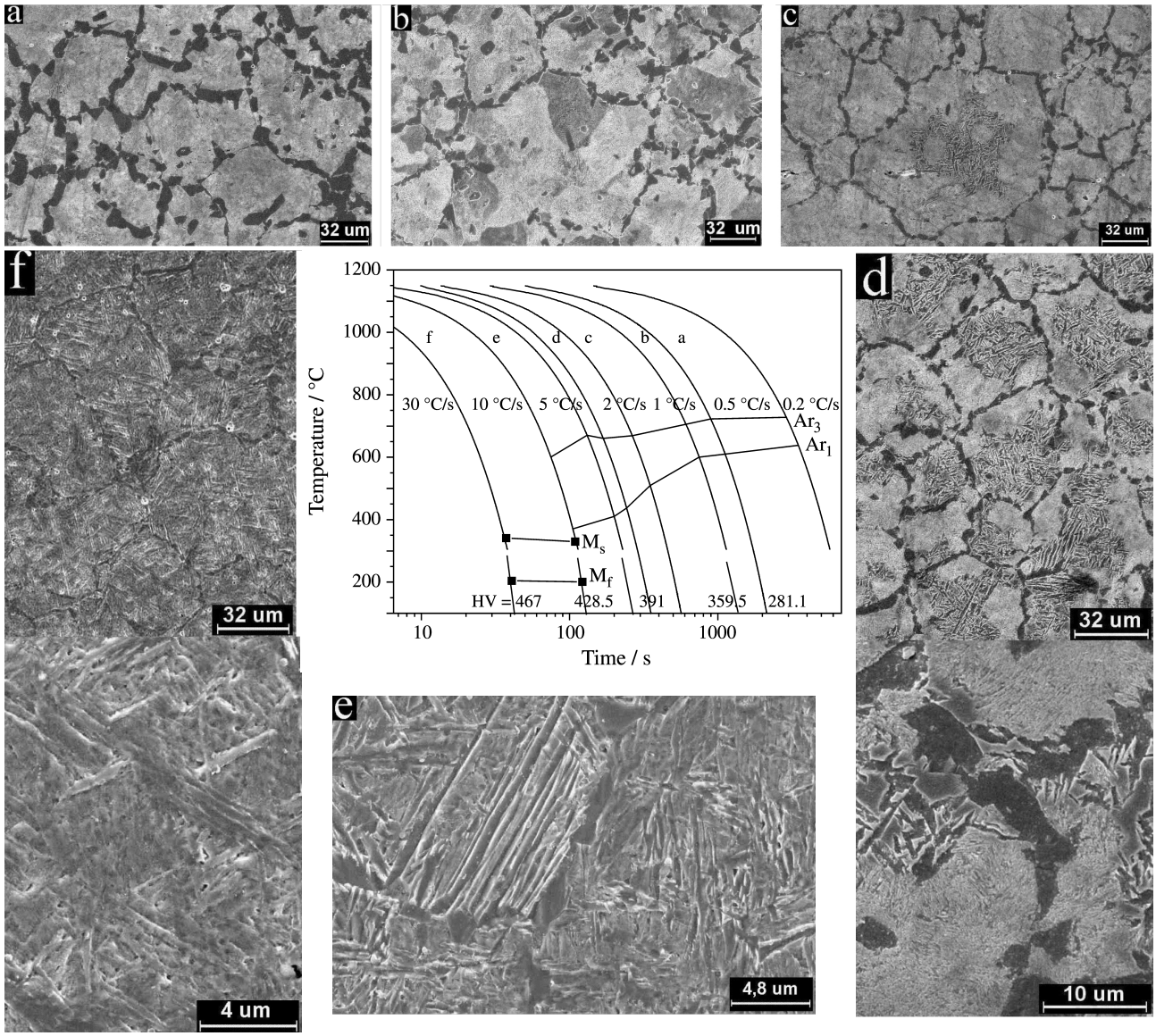

Figure 2. Microstructures observed after cooling to room temperature, and Continuous Cooling Transformation diagram determined by dilatometry.

$$\dot{\varepsilon}\, e^{Q/RT} = A\,[\,\sinh(\alpha\,\sigma)\,]^n = Z$$

where $\dot{\varepsilon}$ is the strain rate; σ the peak stress; Q the activation energy for hot deformation; T the temperature; A, α, n, and R constants; and Z the Zener-Hollomon parameter. The fit of the experimental data to this equation is depicted in Fig. 6, which indicates a change in slope of the ln[sinh($\alpha\sigma$)] *vs.* 1/T curve, with the transition at 700 °C. The activation energies determined in the high- and low-temperature ranges were 332 and 593 kJ/mol, respectively.

Figures 4 and 6 indicate that the rise in the level of stress and the activation energy are greater at lower temperatures. Based on this observation, the plastic behavior of this steel can be separated into two regions: above and below 700 °C. The increased material strength at temperatures below 700 °C can be attributed to the presence of ferrite and pearlite, while the higher activation energy can be correlated with deformation in the multi-phase region[16,17].

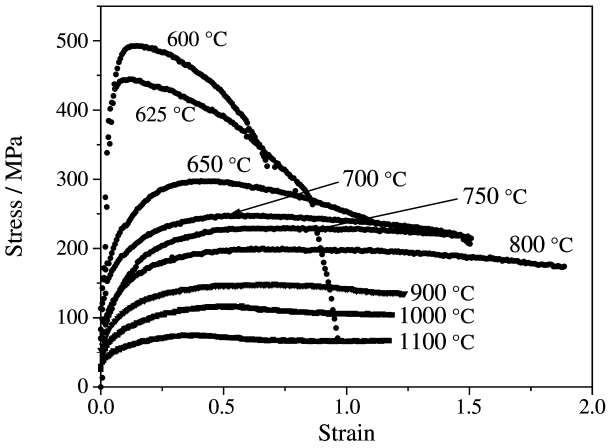

Figure 3. Plastic flow curves determined under isothermal continuous conditions.

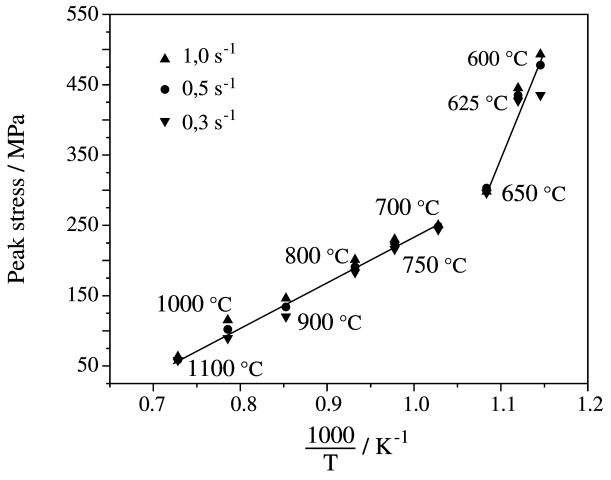

Figure 4. Dependence of the peak stress on deformation temperature.

The influence of microstructural evolution on plastic flow during thermomechanical treatments can be seen more clearly through multiple pass tests under continuous cooling conditions. Figure 7a represents a sixteen pass testing schedule simulating hot plate mills with a cooling rate of 1 °C/s, an interpass time of 30 s, and 15% straining after soaking at 1150 °C. The dependence of the mean flow stress (MFS) on the inverse absolute temperature is shown in Fig. 7b. This figure clearly shows that the level of stress depends on deformation temperature, and that the slope of MFS *vs.* 1/T takes on four different values as deformation temperature is decreased from 1150 °C to 600 °C with transition close to 860 °C, 710 °C and 650 °C.

At high temperatures, full recrystallization takes place and the increase in mean flow stress is solely due to the decrease in temperature. At temperatures below the Tnr (860 °C), there is only partial recrystallization or no recrystallization at all, and the mean flow stress increases more rapidly as temperature decreases. Below 710 °C, the changes in the slope are associated with the beginning of

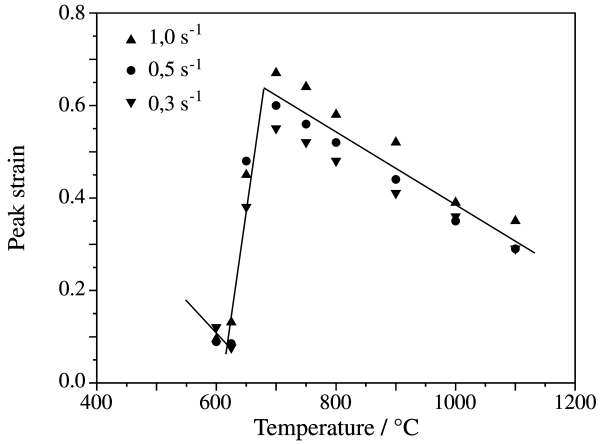

Figure 5. Dependence of the peak strain on deformation temperature.

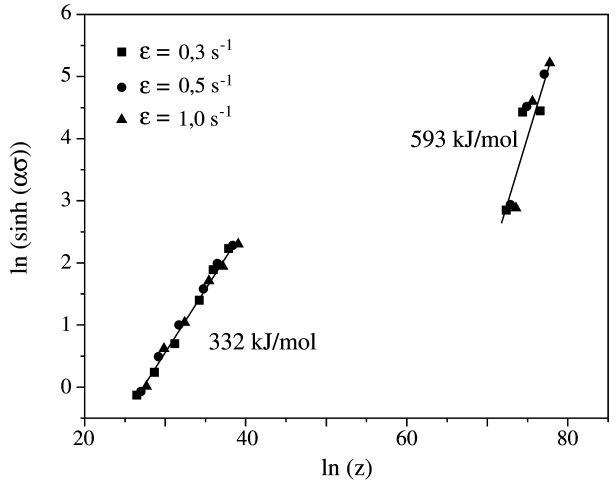

Figure 6. Dependence of the peak stress on the Zener-Hollomon parameter, suggesting two different plastic behaviors for this steel.

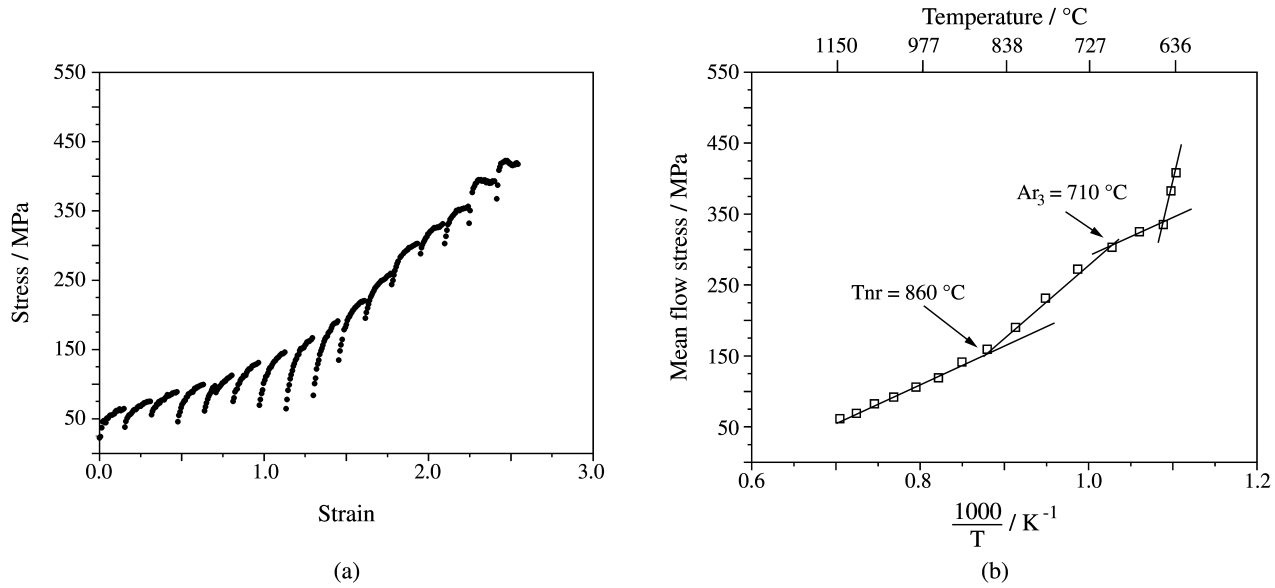

Figure 7. Stress-strain curves (a) and mean flow stress-inverse straining temperature curve (b) for samples deformed under continuous cooling conditions.

the formation of pro-eutectoid ferrite and pearlite. The mean flow stress increases less rapidly because ferrite is softer than austenite and, at lower temperatures, there is a sharp increase as pearlite begins to form.

Plastic behavior at low temperatures was investigated using double isothermal straining tests; Figure 8 displays data from tests performed at 750 °C, 700 °C and 650 °C. Some softening occurred in the interpass time at 750 °C, but the level of stress was greater in the second straining than it was in the first. The second deformation stress-strain curves maintained the shape of the first pass at higher temperatures, but there was a sharp change at 650 °C. The stress-strain curves for the first pass were typical for materials that soften by dynamic recrystallization, whereas the second pass was characterized by rapid work hardening followed by extensive flow softening. Figure 9 confirms this trend and indicates that the transition occurred around 650 °C.

Discussion

The equilibrium solution temperature for vanadium nitride in this steel, evaluated from the equation given by Narita[18]: $T_s(K) = 8700/(3{,}63 - \log(V.N))$, is estimated to be 1067 °C. Thus, for all the experiments carried out in this work, austenite with most of the vanadium in solid solution having grain size around 100 μm[10] was subjected to different thermomechanical treatments. Carbonitride precipitation took place upon straining on cooling, depending on the experimental conditions imposed. However, at room temperature, every sample that was cooled at a rate of 1 °C/s shown a ferrite-pearlite microstructure, see Fig. 2.

Precipitation during thermomechanical treatments can be detected by its effects on stress-strain curves; the precipitate hardens the microstructure, increasing the flow stress level. As an example, Fig. 7b shows an increase in the slope of mean flow stress *vs.* inverse of temperature diagram, as deformation temperature drops below the Tnr. In this case, it has been well established that deformation-induced precipitation delays static recrystallization during the holding time between consecutive deformations, leading to the accumulation of deformation from pass to pass[19].

It is worth noting, however, that, in the same range of temperatures, the increase in the slope of peak stress *vs.* 1/T curve is not observed in Fig. 4. In this case, straining was carried out after cooling from soaking temperature to test temperature. Even though straining was applied below the Tnr, precipitation did not occur because static precipitation is rather sluggish. A similar interpretation holds true in the analysis of the role of interpass time in the tests carried out isothermally with double straining. At 700 °C and 750 °C, the level of stress is somewhat higher at the second straining than at the first; here, precipitation took place in the interpass time.

Precipitation during multiple pass deformation affects the behavior of austenite in different ways. During lower temperature hot deformation, precipitation in austenite stabilizes the dislocation substructure, inhibiting the restoration processes. The stored energy expands the potential nucleation sites and raises the Ar_3. On the other hand, as precipitation takes place in austenite, less vanadium is left in solution, which decreases the hardenability of austenite and gives rise to the gamma-alpha transformation. A comparison of the temperatures measured for the startup of austenite transformation into ferrite without straining (dilatometric technique) against those with straining (multiple

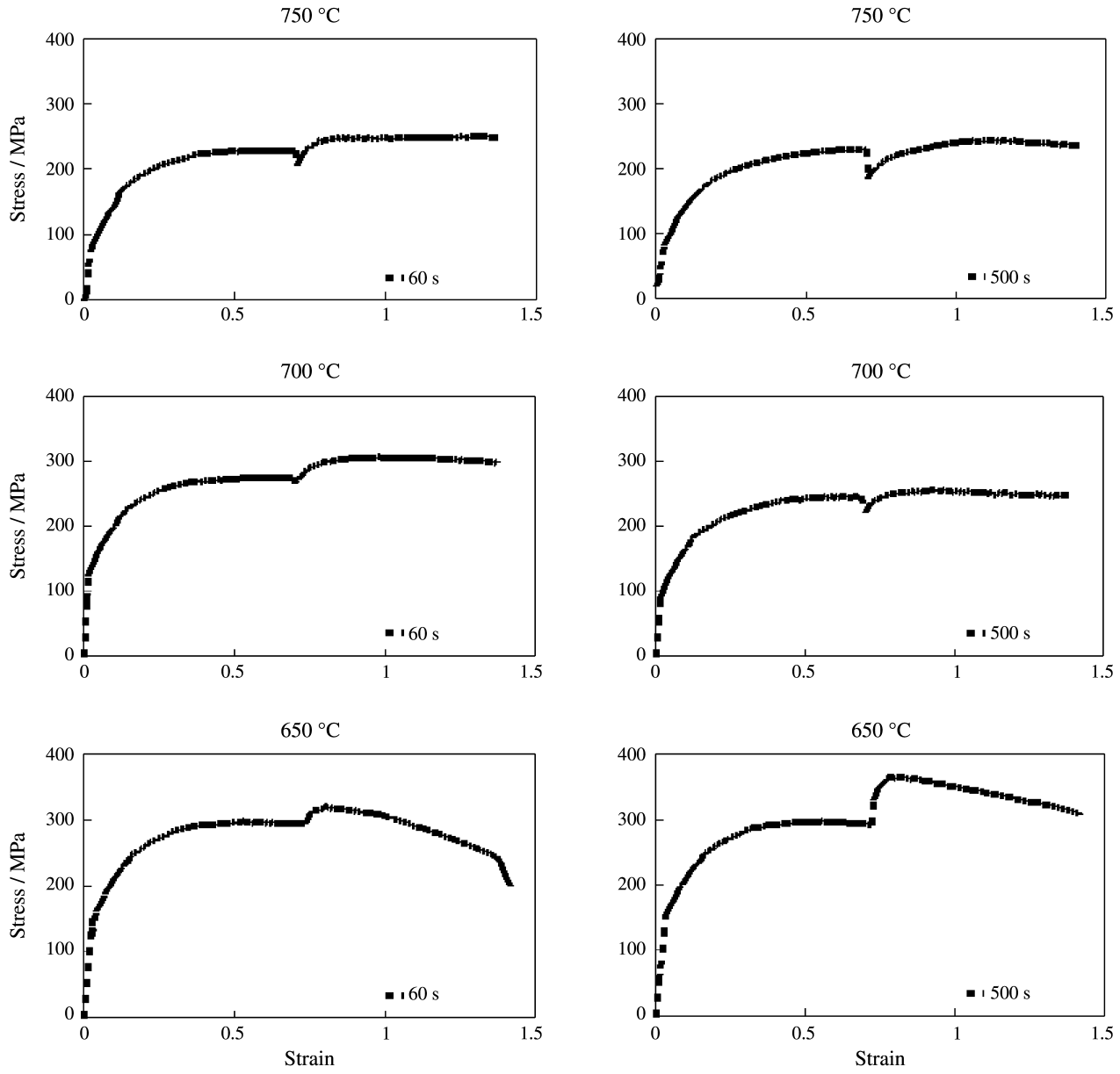

Figure 8. Flow curves of isothermal double straining tests at 750 °C, 700 °C and 650 °C with interpass time of 60 s and 500 s.

straining) under continuous cooling conditions, showed that the expected difference was not achieved. Both data indicate similar values, *i.e.*, around 710 °C. Bearing in mind that this steel had a high vanadium, carbon and nitrogen content, certainly the potential for carbonitride precipitation is not spent during austenite deformation, and interphase precipitation does take place during transformation. Thus, interphase precipitation during transformation can retard the progress of transformation by pinning interfaces.

Although precipitation has been observed by electron microscopy in pearlitic ferrite lamellas in medium carbon vanadium microalloyed steels[20], it proved impossible to distinguish its effect in this study because both pearlite formation and carbonitride precipitation increase the level of stress. Along with increasing stress, the presence of pearlite during straining changes the shape of the flow stress. The sharp increase in the level of stress at the beginning of straining can be associated with pearlitic cementite lamellas, which is a hard phase and maintains an orientation relationship of the Kurdjumov-Sachs type with part of the pearlitic ferrite lamellar interfaces. This coherence increases the degree of interaction between the cementite and the glide dislocation. During the initial stages of deformation, the harder phase thus inhibits deformation of the softer one, increasing yield stress as well as the work-hardening rate. The flow softening after peak stress can be

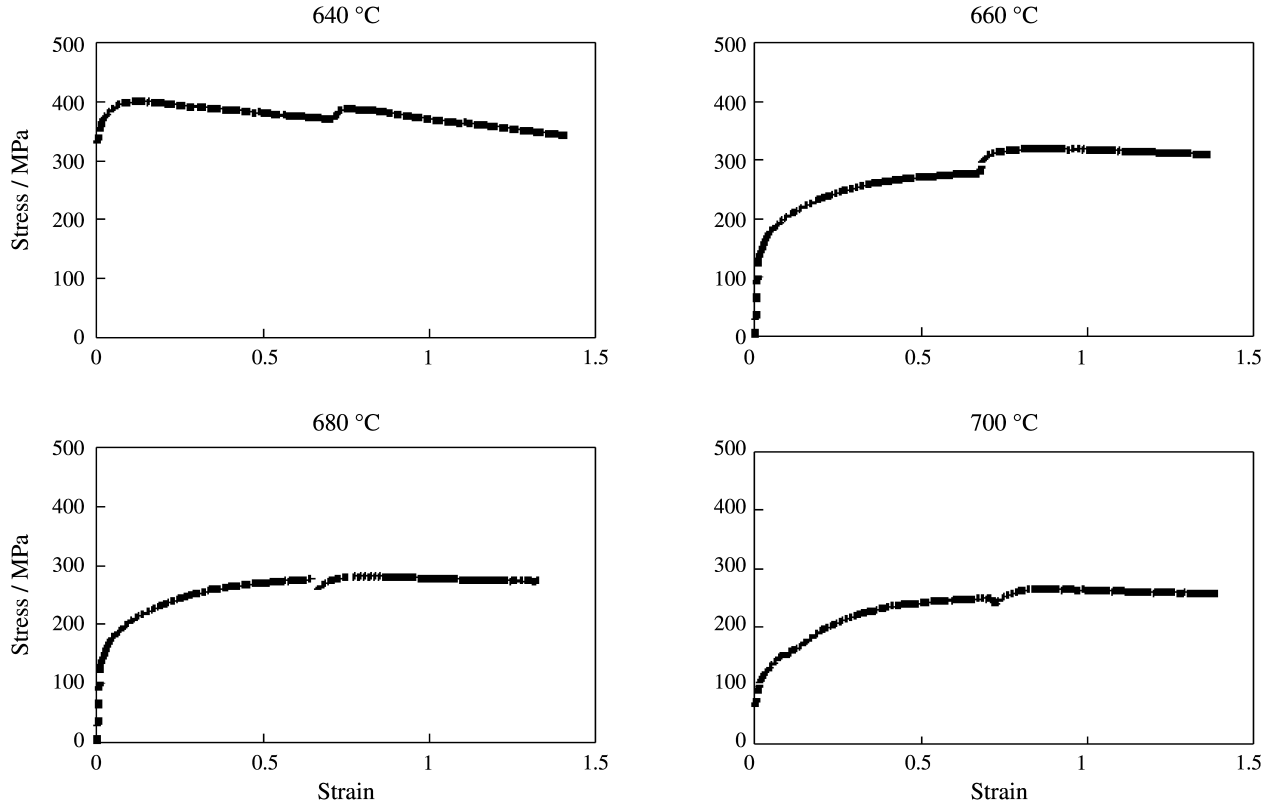

Figure 9. Flow curves of double straining tests over the temperature range of 640 °C to 700 °C with interpass time of 300 s.

associated with epheroidization[21] and/or breakage of the perlitic cementite lamellas, along with the loss of coherence as straining progresses[17].

Conclusions

In the austenite field, the medium carbon vanadium microalloyed steel studied here displayed stress-strain curves with the characteristic shape expected for materials that soften by dynamic recrystallization, and exhibiting an activation energy for hot deformation of 332 kJ/mol was found.

When subjected to a deformation schedule under continuous cooling conditions, this steel showed the no recrystallization temperature at 860 °C, indicating that deformation-induced precipitation took place within the austenite field.

Similar values measured for Ar_3 with and without straining suggest that interphase precipitation occurred during transformation, retarding the progress of transformation by pinning interfaces.

At low hot working temperatures, when the microstructure consisted of pro-eutectoid ferrite and pearlite, the flow curves had a peculiar shape: rapid work hardening to a hump, followed by an extensive flow-softening region.

Acknowledgements

The financial support of the Brazilian research funding agencies FAPESP and CNPq is gratefully acknowledged.

References

1. Wright, P.H. *Advanced Materials Processes*, v. 12, p. 29-34, 1988.
2. Tostenson, D.; Bertolo, R.; Glasgal, B. *Fundamentals and Application of Microalloying Forging Steels*, Tyne, C. J.; Krauss, G.; Matlock, D.K., eds., TMS (Minerals, Metals & Materials Society), p. 327-344, 1996.
3. Meyer, L.; Müschenborn, W.; Schriever, U. *Thermomechanical Processing in Theory, Modeling and Practice*, Hutchinson, B.; Andersson, M.; Engberg, G.; Karlsson, B.; Siwecki, T., eds., ASM Sweden, Stockholm, p. 93-120, 1996.
4. Engineer, S.; Huchtemann, B.; Schüler, V. *Steel Research*, v. 58, p. 369-376, 1987.
5. Peñalba, F.; Zapiráin, F.; Carsí, M.; Garcia de Andrés, C.; Andrés, M.P. *Mater. Sci. Forum*, v. 94-96, p. 689-696, 1992.
6. Medina, S.F.; Lopez, V. *ISIJ Int.*, v. 33, p. 605-614, 1993.
7. Santos, J.M.R. *Tese de Doutorado*, Universidade Federal de São Carlos, 1997.
8.

Quispe, A.; Medina, S.F.; Valles, P. *ISIJ Inter.*, v. 37, p. 783-788, 1997.

9. Revidriego, F.J.; Abad, R.; López, B.; Gutiérrez, I.; Urcola, J.J. *Scri. Mater.*, v. 34, p. 1589-1594, 1996.
10. Souza, R.C. *Tese de Doutorado*, Universidade Federal de São Carlos, 1996.
11. Peñalba, F.; Garcia de Andrés, C.; Carsí, M.; Zapirain, F.J. *Mater. Sci.*, v. 31, p. 3847-3852, 1996.
12. Zhang, F.; Boyd, J.D. *Fundamentals and Applications of Microalloying Forging Steels*, Tyne, C.J.; Krauss, G.; Matlock, D.K., eds., TMS (Minerals, Metals & Materials Society), p. 127-141, 1996.
13. Dong, H.; Li, G.; Lu, Z. *Fundamentals and Application of Microalloyed Forging Steels*, Tyne, C. J.; Krauss, G.; Matlock, D. K., eds., TMS (Minerals, Metals & Materials Society), p. 549-560, 1996.
14. Jorge Jr., A.M.; Balancin, O. *Revista de Engenharia e Ciências Aplicadas*, v. 2, p. 133-137, 1994/1995.
15. Sellars, C.M.; McG.Tegart, W.J. *Mem. Sci. Rev. Metall.*, v. 63, p. 731-740, 1966.
16. Briottet, L.; Jonas, J.J.; Montheillet, F. *Acta Mater.*, v. 44, p. 1665-1672, 1996.
17. Balancin, O.; Hoffmann, W.A.M.; Jonas, J.J. *Metall. Mat. Trans.*, v. 31A, p. 1353-1364, 2000.
18. Narita, K. *ISIJ Int.*, v. 15, p. 145-153, 1975.
19. Borato, F.; Barbosa, R.; Yue, S.; Jonas, J.J. *THERMEC-88*, Tamura, I., ed., Tokyo, v. 1, p. 383-390, 1988.
20. Edmonds, D.V. *Fundamentals and Applications of Microalloying Forging Steels*, Tyne, C.J.; Kraus, G.; Matlock, D.K., eds., TMS (Minerals, Metals & Materials Society), p. 111-125, 1996.
21. Harrigan, M.J.; Sherby O.D. *Mater. Sci. Eng.*, v. 7, p. 177-189, 1971.

FAPESP helped in meeting the publication costs of this article